Resistance behavior and magnetization reversal analysis of individual Co nanowires

B. Leven* and G. Dumpich
Institut für Physik, Universität Duisburg-Essen, 47048 Duisburg, Germany
(Received 10 September 2004; published 23 February 2005)

Since the direct observation of magnetization reversal processes in nanostructured systems is hard to achieve, we use magnetoresistance measurements as an indirect sensing tool. To avoid dipolar interactions present in nanowire gratings individual Co nanowires are prepared by electron beam lithography on Si substrates. Using a special two step process nonmagnetic gold contacts are attached to the Co nanowires to exclude an influence of the contact structures on the magnetization reversal process. To support the magnetoresistance analysis also the structure and morphology as well as the magnetic properties of the Co nanowires have been characterized using various microscopy and measurement techniques. Depending on the direction of the applied field three different magnetoresistance measurements can be distinguished. Based on the anisotropic magnetoresistance effect the transversal and the polar magnetoresistance reflect a coherent rotation of the magnetization independent of the wire width. In contrast, the longitudinal magnetoresistance shows a wire widths dependence of the magnetization reversal processes. In small wires nucleation processes occur whereas in wide wires the formation of complex domain structures has been observed. Nanowires with a width in between these groups show "transition"-like reversal processes.

DOI: 10.1103/PhysRevB.71.064411 PACS number(s): 73.61.−r, 75.60.Ej, 75.60.Ch

INTRODUCTION

The investigation of spin dependent transport phenomena is fundamental for the development and application of magnetoelectronics.[1] One example is the giant magnetoresistance effect (GMR) which is caused by spin dependent scattering of electrons at the interfaces of exchange coupled multilayer systems.[2] Other spin dependent transport phenomena are, e.g., the anisotropic magnetoresistance (AMR) and the domain wall magnetoresistance (DWMR). The AMR is caused by an anisotropic scattering of electrons and depends strongly on the orientation of the magnetization related to the current direction. The physical origin of the AMR is the spin orbit interaction.[3] The DWMR is caused by scattering effects of electrons at the domain walls and can be ascribed to two different origins: (1) How well the precession of the electron spins overlaps with the local variation of the exchange field while passing through the domain wall, and (2) spin dependent scattering in the domain walls as has been described for the giant magnetoresistance (GMR) effect.[4,5] The DWMR is of increasing interest since it causes additional resistance contributions during the magnetization reversal process in micro- and nanostructured systems.[6] In particular, the formation of domain walls and their pinning behavior is of basic interest.[7–11] The main goal is to get a better understanding of magnetization reversal processes from the micromagnetic point of view and thus being able to design special features of magnetic devices on the nanometer scale. For the experimental investigation of magnetization reversal processes on the nanometer scale it has to be taken into account that the magnetic moment of an individual structure is so small that it cannot be detected by means of macroscopic methods as, e.g., SQUID or MOKE. Therefore, to characterize the magnetization behavior of nanostructures a high number of identical structures have to be analyzed.[12–19] However, the major disadvantage in investigating arrays of nanostructures is the existence of dipolar interactions between neighboring structures which might influence the reversal mechanism. Recently, to exclude these disturbing effects, new methods have been developed to investigate individual nanostructures. E.g., Micro-SQUIDS[7] and Hall-micromagnetometry[21] are used to measure M(H)-hysteresis loops. To image the domain structure Kerr microscopy,[22] MFM,[23–25] Lorentz microscopy[9,26,27] and spinpolarized STM[28–30] is used. Furthermore, magnetoresistance measurements have been found to be well qualified to investigate the magnetization reversal processes in nanostructures,[6,12,13,20] since the AMR is sensitive to the magnetization distribution during the reversal process. This has also been shown for individual nanostructures.[31–33,35,36] However, when using ferromagnetic contacts these contact structures influence the reversal mechanism.[37] To definitely exclude a magnetic influence of the contacts on the individual ferromagnetic nanowires we use nonmagnetic gold contacts for our experiments which allow us to investigate the pure magnetization reversal behavior of individual Co nanowires.

EXPERIMENT

The individual nanowires have been prepared using a special two step electron beam lithography technique (EBL) in combination with electron beam evaporation of Co. To avoid surface oxidation of the Co we evaporate in situ a thin Pt cap layer with a film thickness of $t_{Pt}=2$ nm during the first EBL step. In the second EBL step nonmagnetic gold contacts are attached precisely to the individual Co nanowires. The general dimensions of the nanowires are a length of $l=40$ μm, a film thickness of $t_{Co}=30$ nm and varying wire widths of $w=100$ nm…10 μm. In Fig. 1 a typical sample structure is shown obtained by scanning electron microscopy. On the left hand side two rows of four gold contact pads are shown, each providing the electrical contacts of one individual nanowire to carry out 4 point probe resistance measurements. On

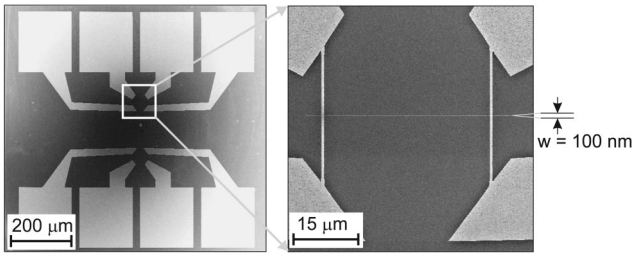

FIG. 1. SEM pictures of a typical sample structure: (a) overview and (b) enlarged area of a 100 nm wide Co wire and the gold contact structure.

the right hand side a 100 nm wide Co nanowire is shown at an enlarged scale.

Structural and morphological analysis of the samples have been carried out using various methods: scanning electron microscopy (SEM), atomic force microscopy (AFM), scanning tunneling microscopy (STM), transmission electron microscopy (TEM) and electron diffraction. SEM and AFM investigations reveal, that the profile of the nanowires is rectangular and that a variation of the wire width of $\delta w \simeq \pm 7$ nm occurs independent on the wire width. From STM investigations we obtain a surface roughness of $\delta t \simeq \pm 3$ nm. For TEM investigations we prepare the nanowires on top of carbon capped sodium substrates which are finally dissolved in water. We find that the Co film is polycrystalline and the mean grain size is about $\Phi \simeq 7$ nm. The small grain size gives an upper limit for the mean free path of the conduction electrons since $l_e \leqslant 7$ nm. Thus, the classical Lorentz magnetoresistance can be neglected as will be discussed below. Furthermore, it is found that the Co film is not textured. This means that the magnetic easy axis of the Co grains in the polycrystalline film is randomly distributed and can be neglected in average. The crystal structure is determined by means of electron diffraction and is mainly hcp Co.

MAGNETIC PROPERTIES

To characterize the magnetic properties of the nanowires we investigated the domain structure using magnetic force microscopy (MFM) and Kerr microscopy at room temperature. In Fig. 2 MFM images of the remanent state of single Co nanowires with different widths are shown exemplarily. The images reflect the remanent magnetization state after a magnetic saturation parallel to the wire axis in an external magnetic field of $B=2$ T. As the MFM tip is only sensitive to the stray fields perpendicular to the film plane, dark and bright contrasts show areas where the stray fields escape out of the film plane or penetrate into the film plane. As shown in Fig. 2 the remanent state of wires with widths $w \geqslant 2$ μm is characterized by a complex multidomain state. The strong dark and bright contrast at opposite domain boundaries indicates that the magnetization is predominantly aligned in plane, as has been confirmed by Kerr microscopy.[46] In contrast, smaller Co wires ($w \leqslant 1$ μm) show a monodomain remanent state, as can be seen in Fig. 2. The $w=1$ μm wide wire as well as the $w=300$ nm wide wire shows almost no contrast along the wire. Only at the wire ends a bright and a

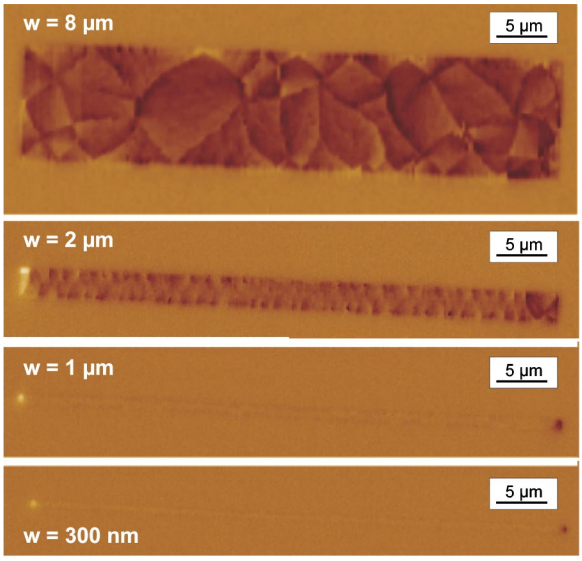

FIG. 2. (Color online) Magnetic force micrographs of the remanent state of single Co nanowires with different wire widths: $w=8$ μm, $w=2$ μm, $w=1$ μm, and $w=300$ nm. Prior the wires have been saturated magnetically in an external field of $B=2$ T.

dark spot occurs. This means that only one domain exists in the whole nanowire in which the magnetization is aligned in plane parallel to the wire axis. This axis is the magnetic easy axis of the system, which has been confirmed by SQUID investigations.

To further characterize the magnetometric properties of the Co nanowires by means of SQUID, gratings of 16000 single nanowires have been prepared. We apply the magnetic field in three different directions with respect to the wire axis: (1) in plane parallel to the wire axis, which is called the longitudinal direction, (2) in plane perpendicular to the wire axis, the so-called transversal direction, and (3) out of plane, the so-called polar direction. Figure 3 shows typical normalized $M(B)$-hysteresis loops for all three different field directions measured at a temperature of $T=5$ K. The wire width in the investigated grating is $w=550$ nm and the distance be-

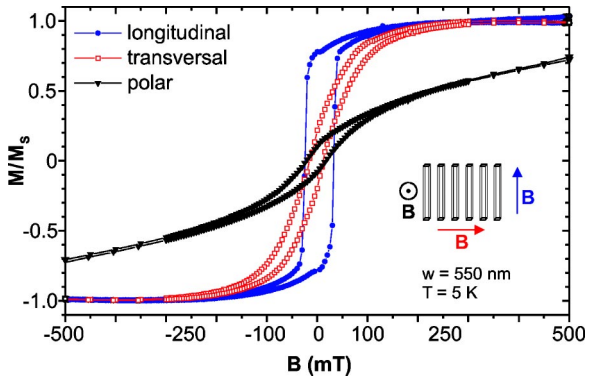

FIG. 3. (Color online) Normalized $M(B)$-hysteresis curves of a Co nanowire array with a wire width of $w=550$ nm and a periodicity of $d=5$ μm measured at $T=5$ K. The field is applied in a longitudinal (dots), transversal (squares), and polar (triangles) direction.

tween the single wires is $d=5\ \mu$m. This large distance is chosen to markedly reduce the dipole coupling.[12]

The results of the longitudinal measurement is given by the dots, the open squares give the results of the transversal measurement and the triangles the results of the polar measurement. As can be seen in Fig. 3 the $M(B)$-hysteresis loop obtained in longitudinal geometry shows a nearly rectangular shape which indicates that the long axis of the wire is the magnetic easy axis. On the other hand, the shape of the hysteresis loops measured in transversal and polar geometry are much more rounded with much lower magnetization gradients. This indicates that two different magnetic hard axes of the Co nanowires exist. Comparing the $M(B)$-hysteresis loop taken along one of the magnetic hard axes to that taken along the magnetic easy axis, the effective magnetic anisotropy energy density can be estimated using normalized $M(B)$ plots from Fig. 3.[39] In doing so, the anisotropy energy density based on the transversal measurement is $E_{trans}\sim 2\times 10^5\ \mathrm{J/m^3}$, while the value deduced from the polar measurement is $E_{polar}\sim 1\times 10^6\ \mathrm{J/m^3}$. The occurrence of the magnetic anisotropy can originate from the shape (shape anisotropy due to demagnetizing effects), the crystal structure (magnetocrystalline anisotropy) and other factors.[39] For the present measurements we can neglect the magnetocrystalline aniostropy since we find from our TEM investigations that the small grains are randomly oriented exhibiting no film texture. Thus, the shape anisotropy is the dominating factor which strongly depends on the direction of the magnetic field (longitudinal, transversal or polar), since the width of the nanowires is much smaller than the wire thickness. This explains the large ratio of the anisotropy energy densities $E_{trans}:E_{polar}=1:5$ as obtained analyzing the data in Fig. 3.

Additionally, from the SQUID measurements we reveal an absolute magnetic saturation moment of the nanowire grating ($w=550$ nm) of $m\simeq 1.5\times 10^{-8}\mathrm{Am^2}$. Since we know the Co volume of the sample, this leads to a saturation magnetization of $M_s=1385$ kA/m, which is about 95% of the literature value. Based on this result we suggest that the in situ coverage of the Co nanowire surface with a 2 nm thick Pt layer succeeds in minimizing oxidation effects, as have been detected for non capped Co wires.[38]

MAGNETORESISTANCE AND MAGNETIZATION REVERSAL

As discussed above, magnetoresistance measurements can be used as a tool to determine the magnetization reversal process of individual wires. The clear correspondence of the magnetoresistance to the magnetization reversal is demonstrated in Fig. 4. The upper graph in Fig. 4 shows a typical $M(B)$-hysteresis curve of a nanowire grating ($w=550$ nm) measured in a longitudinal applied magnetic field at a temperature of $T=5$ K. The lower graph shows a typical longitudinal magnetoresistance curve of an individual Co nanowire of comparable width ($w=634$ nm) measured at a temperature of $T=4.2$ K for small magnetic fields $-300\ \mathrm{mT}\leqslant B\leqslant 300$ mT. As can be seen in Fig. 4 the magnetoresistance shows a hysteretic behavior with pronounced minima marking switching fields, which are—as compared

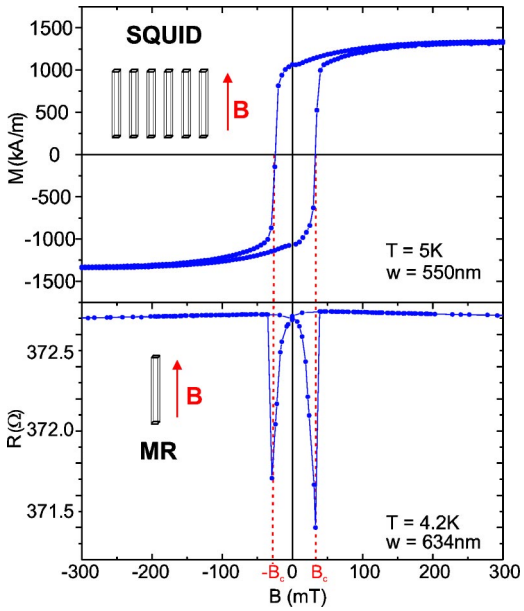

FIG. 4. (Color online) Comparison of a $M(B)$-hysteresis curve of a Co nanowire array and the longitudinal magnetoresistance of a single Co nanowire of comparable width.

to the $M(B)$ curve above—identical to the coercive fields indicated by the dashed lines. This example emphazises the close relationship between the SQUID results and the magnetoresistance with respect to the magnetization reversal behavior. The origin of the resistance minima at the coercive fields is related to AMR effects[36] and will be discussed in more detail below.

First, we discuss the *transversal magnetoresistance* to analyze the magnetization reversal process when the magnetic field is applied parallel to one hard magnetic axis of the system. In Fig. 5 the transversal magnetoresistance of an individual Co nanowire is shown ($w=120$ nm, $T=4.2$ K). The magnetic field is applied in plane perpendicular to the wire axis. The arrows indicate the measurement procedure. Starting at a resistance value of $R=5101\ \Omega$ in the remanent state ($B=0$ mT), which is characterized by MFM as a monodomain state with all magnetic moments being aligned parallel to the wire axis, the resistance continuously decreases with increasing field and reaches a constant value for high

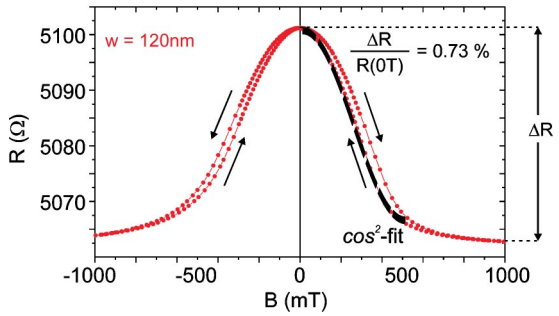

FIG. 5. (Color online) Transversal magnetoresistance of a 120 nm wide Co nanowire measured at $T=4.2$ K. The black dashed line shows a $\cos^2\alpha$ fit indicating a coherent rotation of the magnetic moments during the reversal process.

magnetic fields $|B| \geqslant 1000$ mT in the saturation regime. Decreasing the magnetic field from saturation the transversal resistance increases again and reaches the same remanent resistance value (at $B=0$ mT). The analogous resistance behavior is obtained for the reversed field direction. Note that a small hysteresis occurs, which will be discussed below. The total resistance decrease is $\Delta R/R(0\ \mathrm{T}) = 0.73\%$, which indicates that this behavior is due to the AMR effect. To analyze the transversal resistance in more detail the data have been fitted with a $\cos^2(B)$ profile, as indicated by the black dashed line in Fig. 5. The good agreement between the experimental data and the fit confirms that the transversal magnetoresistance is due to AMR reflecting a coherent rotation of the magnetic moments from the longitudinal (magnetic easy) axis to the transversal (magnetic hard) axis. The small hysteresis of the magnetoresistance occurs since the rotation process is influenced by the shape anisotropy. When the transversal magnetic field is increased (see arrow) the magnetization rotation is hindered due to the transition from the magnetic easy to the hard axis. In contrast, reducing the field, the shape anisotropy supports the magnetization rotation. This behavior is independent on the wire width and has also been observed when the magnetic field was applied in the polar direction. This means that in the present nanowires the magnetization reversal process between the magnetic easy axis and a magnetic hard axis in general can be described by coherent rotation. To quantify these results we analyze the $R(B)$ curve measured in transversal applied field using the relation between the resistance $R(B)$ and the anisotropy constant K_u as given in Ref. 48

$$R(B) = R_{\parallel} - (R_{\parallel} - R_{\perp})\left(\frac{M_s B}{2\mu_0 K_u}\right)^2. \qquad (1)$$

In Eq. (1) $R_{\parallel}$ is the resistance measured when all magnetic moments are aligned parallel to the wire axis, in our case $R(B=0\ \mathrm{mT})$ for the 120 nm wide wire. $R_{\perp}$ is the resistance measured when all magnetic moments are aligned transversal to the wire axis, in our case $R(B=1000\ \mathrm{mT})$. M_s is the saturation magnetization and $\mu_0 = 4\pi \times 10^{-7}$ Vs/Am the magnetic permeability constant. We reveal $K_{u1} = 3.2 \times 10^5$ J/m^3 for the magnetization transition from parallel to transversal alignment and $K_{u2} = 2.7 \times 10^5$ J/m^3 for the magnetization transition from transversal to parallel alignment. These values are in good agreement to the transversal anisotropy energy density obtained evaluating the SQUID data. In addition, these results allow to deduce the contribution of the shape anisotropy, which hinders and supports the magnetization rotation, respectively. Assuming, that both effects are equal, we can estimate this anisotropy contribution to $\Delta K = 0.5 \times (K_{u1} - K_{u2}) = 2.5 \times 10^4$ J/m^3 which is about 8% of the transversal anisotropy energy density.

Next, we discuss the *longitudinal magnetoresistance*, which is obtained when the magnetic field is applied parallel to the wire axis and therefore parallel to the current direction. In Fig. 6 the longitudinal magnetoresistance for six single Co nanowires of widths between $w=120$ nm and $w=10$ μm measured at a temperature of $T=4.2$ K is shown. The arrows exemplarily plotted in the resistance curve of the smallest

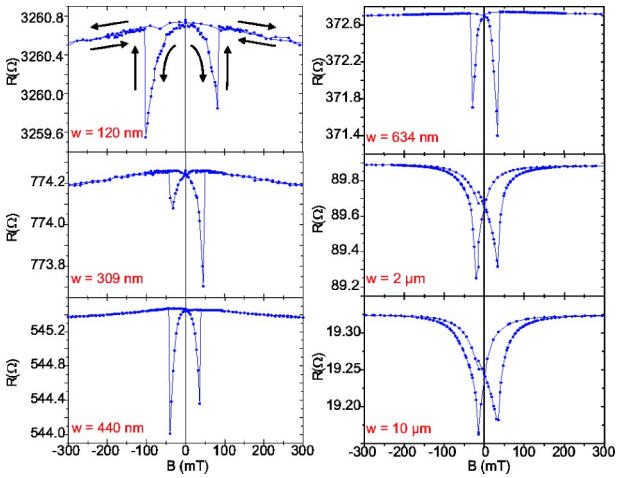

FIG. 6. (Color online) Longitudinal magnetoresistance of single Co nanowires with different widths ($T=4.2$ K). The arrows sketch the measurement procedure. Note that the nonclosed curve in the case of the two widest wires is an experimental artefact and has no physical origin.

wire indicate the measurement procedure. For high magnetic fields $|B| > 300$ mT the resistance is almost constant. For low magnetic fields $|B| < 100$ mT the resistance first continuously decreases followed by a sudden jump to the saturation values. This hysteretic behavior reflects the magnetization reversal process as shown in Fig. 4. The general resistance behavior shown in Fig. 6 can qualitatively be explained as arising from the AMR effect.[36] For Co wires with widths $w \leqslant 1$ μm the resistance value in remanence is almost the same as in saturation as expected from MFM investigations since the magnetization is aligned parallel to the wire axis (see Fig. 2). Further reducing the magnetic field causes a distinct decrease of the longitudinal resistance until the coercive field is reached. This behavior can be described by means of the AMR as formation of domains where the magnetization is oriented perpendicular to the current direction. The abrupt resistance jump to the saturation resistance indicates that these domains suddenly unsnap from their nucleation sites, as confirmed by Kerr microscopy.[46] This interpretation of the magnetoresistance behavior is additionally supported by Monte Carlo simulations carried out for the present Co nanowires.[40,41]

While the shape of the resistance curve remains nearly identical up to wire widths of about $w=634$ nm, it obviously changes in the case of wider Co nanowires ($w=2$ μm, $w=10$ μm). As one can see in Fig. 6 the resistance in remanence of wider Co wires ($w \geqslant 2$ μm) is considerably reduced as compared to the saturation value. Since we know from MFM investigations that the remanent state of nanowires of these widths is characterized by a multidomain configuration (see Fig. 2), this decrease can be described as originating from the formation of domains with transversal magnetization. Note, that the resistance of wider Co nanowires—in contrast to small wires—gradually increases for magnetic fields higher than the coercive field ($|B| > |B_c|$). This resistance behavior denotes that in the case of wide Co nanowires the magnetization reversal process is given by the formation

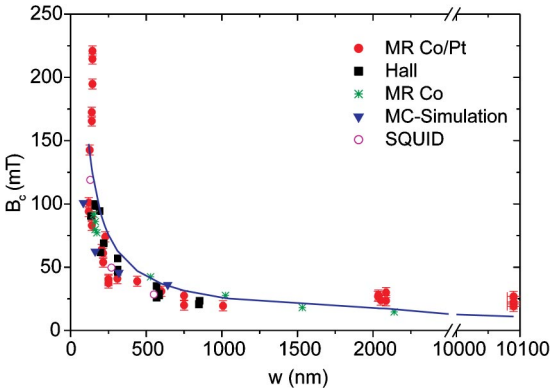

FIG. 7. (Color online) Wire widths dependence of the coercive field summarizing different measurement methods. Dots, stars: resistance measurements of single Co nanowires; circles: SQUID measurements of nanowire gratings; squares: stray field measurements (Ref. 42); triangles: Monte Carlo simulations (Ref. 41). The line is a fit to all data points.

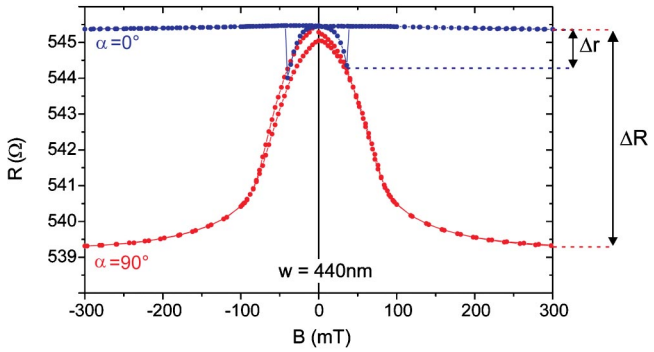

FIG. 8. (Color online) Comparison of the longitudinal (blue dots) and transversal (red squares) magnetoresistance of a 440 nm wide Co nanowire measured at $T=4.2$ K.

of complex domain structures, as has been confirmed by Kerr microscopy and Monte Carlo simulations.

As one can also see from Fig. 6 for each sample the amplitude of the resistance minima is different for negative and positive applied fields, respectively (extremely for the $w=309$ nm wide sample). This can be understood as follows: First, the domain structure at $+B_c$ and $-B_c$ are not expected to be identical. Second, the resistance is measured for field step sizes of $\Delta B \geqslant 2$ mT in time intervals of a few seconds, so that the resistance might change within two measurement steps.

Figure 6 also shows that the position of the resistance minima and thus the coercive field decreases with increasing wire widths. To analyze the wire widths dependence of the coercive field the values of B_c taken from the longitudinal resistance measurements (dots, stars) are plotted in Fig. 7 as a function of the wire width w in combination with various experimental and theoretical results. We thus include in Fig. 7 data obtained from stray field measurements (squares) using Hall bar structures carried out for single Co nanowires,[42] and results of SQUID measurements on nanowire gratings (open circles). Additionally, values received from Monte Carlo simulations carried out for single Co nanowires[41] (triangles) are plotted in Fig. 7. Note, that all experimental methods on individual Co nanowires and SQUID measurements on nanowire gratings, as well as the Monte Carlo simulations[41] display the same wire widths dependence of the coercive field. As can be seen in Fig. 7, the data can be fitted with a single hyperbolic function given by Eq. (2):[47]

$$B_c(w) = B_c(w \to \infty) + \frac{\mu_0}{\pi} M_s t \frac{1}{w}. \qquad (2)$$

$B_c(w \to \infty)$ is the coercive field of a Co film, M_s is the saturation magnetization, $t=30$ nm is the film thickness, and w the width of the nanowires. The physical origin of the observed wire widths dependence of the coercive field are demagnetizing effects, which give rise to the shape anisotropy of the nanowire. Fitting the data with Eq. (2) we obtain a saturation magnetization of $M_s \simeq 1380$ kA/m and the coercive field of a Co film of $B_c(w \to \infty) \simeq 10$ mT. This value agrees very well with the saturation magnetization obtained by SQUID investigations and is also close to the literature value. This means that the volume of the ferromagnetic material has not been significantly reduced by oxidation effects. From this we conclude that the *in situ* coverage of the nanowires with a 2 nm thick platinum layer succeeds in minimizing a surface oxidation.

As discussed above the position of the resistance minima (see Fig. 6) provide the determination of the coercive fields. The interpretation of the *magnitude* of the resistance minima is more complex, since various magnetoresistance contributions might occur and have to be taken into account. To be able to analyze the origin of the magnetoresistance behavior in detail different resistance contributions have to be separated clearly. Using *Kohler's* plot[34] and the revealed residual resistivity ratios $\Gamma = \rho(300\ \mathrm{K})/\rho(4.2\ \mathrm{K})$ of the Co nanowires, which are in the range of $1.32 \leqslant \Gamma \leqslant 1.44$, the resistance contribution due to the classical Lorentz magnetoresistance for typical magnetic fields of $B \leqslant 300$ mT can be estimated to $\Delta R/R \simeq 5 \times 10^{-6}$. This value is of the same order of magnitude as the precision of the resistance measurements and can therefore be neglected for further interpretation. Also, magnetoresistance contributions due to spin disorder scattering can be neglected since the experiments are carried out at low temperatures ($T=4.2$ K).[44,45] Thus, the observed magnetoresistance effects occurring in the Co nanowires are mainly due to AMR and DWMR.

To distinguish between these two effects Fig. 8 shows the longitudinal (dots, $\alpha=0°$) as well as the transversal (squares, $\alpha=90°$) magnetoresistance of a $w=440$ nm wide Co nanowire. As discussed above, in the remanent state of a $w=440$ nm wide Co wire the magnetization is aligned parallel to the wire axis for the longitudinal as well as for the transversal measurement geometry. Thus the total resistance decrease of the transversal magnetoresistance of $\Delta R \simeq 6\ \Omega$ corresponds to an in plane perpendicular magnetization fraction of $M_\perp = 100\%$. On the other hand, the longitudinal magnetoresistance is almost constant, besides the resistance minima at the coercive fields. At $|B| = |B_c|$ the magnitude of the minima in the longitudinal magnetoresistance is $\Delta r \simeq 1.3\ \Omega$.

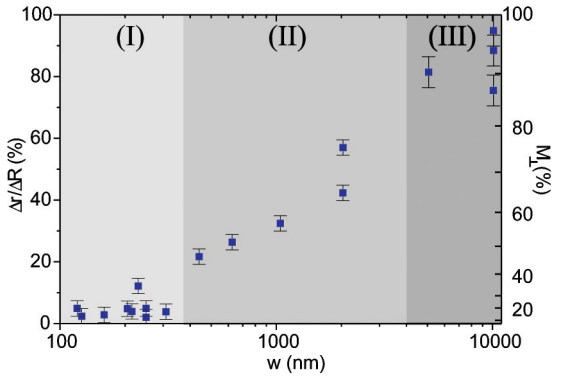

FIG. 9. (Color online) Wire widths dependence of the mean magnitude of the longitudinal magnetoresistance Δr_{av} correlated to the magnetoresistance effect in the transversal magnetoresistance ΔR (see Fig. 8). Additionally, the resultant in plane perpendicular magnetization fraction $M_\perp$ is specified at the right hand scale.

According to the theory of AMR, where the magnetization is related to the square root of the magnetoresistance,[3] we obtain an in plane perpendicular magnetization fraction of $M_\perp \simeq 47\%$ at the coercive field. This result is in good agreement with Monte Carlo simulations ($M_\perp^{sim} \simeq 50\%$)[41] and shows that magnetoresistance contributions arising from DWMR can hardly be detected for the present Co nanowires.

Consequentially, in Fig. 9 the results of this quantitative analysis are summarized. The in plane perpendicular magnetization fraction $M_\perp$ derived from the relative magnitude of the minima of the longitudinal magnetoresistance $\Delta r_{av}/\Delta R$ as mentioned above is plotted as a function of the wire width w. Note, that this quantitative analysis is based on the average magnitude of the longitudinal resistance minima given by $\Delta r_{av} = 0.5 \times [\Delta r(-B_c) + \Delta r(+B_c)]$. Considering the data points displayed in Fig. 9 the results can be separated into three groups: In small Co nanowires with $w \leqslant 230$ nm [group (I)] the perpendicular magnetization fraction is mainly constant and of about $M_\perp \simeq 15\%$. In group (II) ($230\ \text{nm} < w \leqslant 3\ \mu\text{m}$) the perpendicular magnetization fraction increases monotonously with increasing wire width, whereas wide Co nanowires with $3\ \mu\text{m} < w$ [group (III)] show almost constant values of about $M_\perp \simeq 90\%$. These results can be interpreted according to the underlying magnetization reversal processes as follows: The small fraction of perpendicular magnetization obtained for group (I) corresponds to a magnetization reversal process which is characterized by a nucleation process as described above (see Fig. 6). In detail, a vortexlike domain structure nucleates at one or both wire ends, grows with increasing magnetic field and unsnaps when the coercive field is reached. This means that at the coercive field the maximum in plane perpendicular magnetization fraction is obtained. However, as these vortexlike domain structures are only concentrated at the wire ends we would expect a more or less constant in plane perpendicular magnetization fraction as obtained from the magnetoresistance measurements. This magnetization reversal process is in good agreement to Monte Carlo simulations carried out for a single Co nanowire with a width of $w = 84$ nm.[41] In contrast, the quantitative analysis of the resistance data of wires assigned to group (III) reveal again an almost constant, but huge fraction of in plane perpendicular magnetization at the coercive field of $M_\perp \simeq 90\%$. These results indicate that during the magnetization reversal process a complex multidomain state occurs which contains a big amount of in plane perpendicularly oriented magnetic moments. This interpretation is confirmed by MFM (see Fig. 2) and Kerr microscopy investigations[46] of wide wires ($w \geqslant 2\ \mu$m). In the intermediate widths range [group (II)] a monotonous increase of the in plane perpendicular magnetization fraction with increasing wire width is obtained. The underlying magnetization reversal behavior can be described as a "transition" behavior between the two reversal mechanisms discussed for group (I) and (III). This transition behavior is characterized by a nucleation process of vortexlike domain structures at the ends and—in contrast to the mechanism deduced for wires of group (I)—also at the edges of the nanowire, while in the center of the nanowire a domain is conserved in which the magnetization is still aligned parallel to the wire axis favored by the shape anisotropy. This behavior has been revealed from Monte Carlo simulations for a single Co nanowire with a width of $w = 448$ nm,[41] as well as MFM investigations (see Fig. 2). With increasing wire width (and constant wire length and thickness) the influence of the shape anisotropy decreases providing the possibility that also in the center of the nanowire domains with in plane perpendicularly oriented magnetic moments can be formed. Finally, the complex domain structure occurring during the reversal process overbalances the nucleationlike processes as described in the case of wires assigned to group (III).

CONCLUSION

In conclusion, we show that the magnetoresistance of individual Co nanowires is sensitive to the magnetization reversal process. Based on the AMR the transversal magnetoresistance clearly reflects a coherent rotation of the magnetic moments during the reversal process independent on the wire width. On the other hand, the longitudinal magnetoresistance shows that, dependent on the wire width, three different reversal processes can be obtained. In small Co nanowires ($w \leqslant 230$ nm) the magnetization reversal process is characterized by nucleation processes and domain wall propagation in agreement with MFM and Kerr microscopy investigations as well as Monte Carlo simulations. In wide Co nanowires ($w \geqslant 3\ \mu$m) complex domain structures occur effecting the magnetization reversal. For Co wires with widths $230\ \text{nm} < w < 3\ \mu$m a "transition" behavior occurs. However, even if the magnetization reversal process of the individual Co nanowires can qualitatively be sensed by the magnetoresistance behavior based on the AMR, additional domain wall scattering effects cannot be separated. To do so, magnetoresistance investigations of out of plane magnetized nanowires have to be carried out, since these systems provide the clear separation of the domain wall magnetoresistance as has been shown elsewhere.[43] Nevertheless, the magnetoresistance analysis of individual Co nanowires provides detailed information about the occurring magnetization reversal processes for a wide range of wire widths which is hard to detect by direct observation methods.

ACKNOWLEDGMENTS

We are very grateful to Jeffrey McCord and Rudolf Schaefer at the IFW in Dresden for carrying out the Kerr microscopy investigations of the single Co nanowires. We also thank Denise Hinzke and Ulrich Nowak at the Theoretische Physik at the Universität Duisburg-Essen for the intense and fruitful collaboration. This work has been supported by the Deutsche Forschungsgemeinschaft within the SFB 491.

*Current address: Fachbereich Physik, Technische Universität Kaiserslautern, 67663 Kaiserslautern, Germany. Email address: leven@physik.uni-kl.de

[1] G. Prinz and K. Hathaway, Phys. Today **48**, 24 (1995).
[2] S. S. P. Parkin, Phys. Rev. Lett. **71**, 1641 (1993).
[3] R. McGuire and R. I. Potter, IEEE Trans. Magn. **11**, 1018 (1975).
[4] J. F. Gregg, W. Allen, K. Ounadjela, M. Viret, M. Hehn, S. M. Thompson, and J. M. D. Coey, Phys. Rev. Lett. **77**, 1580 (1996).
[5] P. M. Levy and S. Zhang, Phys. Rev. Lett. **79**, 5110 (1997).
[6] K. Hong and N. Giordano, Phys. Rev. B **51**, 9855 (1995).
[7] W. Wernsdorfer, K. Hasselbach, D. Mailly, B. Barbara, A. Benoit, L. Thomas, and G. Suran, Phys. Rev. B **55**, 11 552 (1997).
[8] R. Ferre, K. Ounadjela, J. M. George, L. Pireaux, and S. Dubois, Phys. Rev. B **56**, 14 066 (1997).
[9] T. Schrefl, J. Fidler, K. J. Kirk, and J. N. Chapman, J. Magn. Magn. Mater. **175**, 193 (1997).
[10] U. Nowak and D. Hinzke, J. Appl. Phys. **85**, 4337 (1999).
[11] D. Hinzke and U. Nowak, Phys. Rev. B **61**, 6734 (2000).
[12] S. J. Blundell, C. Shearwood, M. Gester, M. J. Baird, J. A. C. Bland, and H. Ahmed, J. Magn. Magn. Mater. **153**, L17 (1994).
[13] C. Shearwood, S. J. Blundell, M. J. Baird, J. A. C. Bland, M. Gester, and H. Ahmed, J. Appl. Phys. **75**, 5249 (1994).
[14] J. I. Martin, J. L. Costa-Kraemer, F. Briones, and J. L. Vincent, J. Magn. Magn. Mater. **221**, 215 (2000).
[15] J. Meier, B. Doudin, and J.-Ph. Ansermet, J. Appl. Phys. **79**, 6010 (1996).
[16] K. Ounadjela, R. Ferre, L. Louail, J. M. George, J. L. Maurice, L. Pireaux, and S. Dubois, J. Appl. Phys. **81**, 5455 (1997).
[17] D. J. Sellmyer, M. Zheng, and R. Skomski, J. Phys.: Condens. Matter **13**, R433 (2001).
[18] R. P. Cowburn, J. Phys. D **33**, R1 (2000).
[19] T. Schmitte, K. Theis-Broehl, V. Leiner, H. Zabel, S. Kirsch, and A. Carl, J. Phys.: Condens. Matter **14**, 7525 (2002).
[20] J. E. Wegrowe, S. E. Gilbert, D. Kelly, B. Doudin, and J. P. Ansermet, IEEE Trans. Magn. **34**, 903 (1998).
[21] D. Grundler, G. Meier, K.-B. Brooks, Ch. Heyn, and D. Heitmann, J. Appl. Phys. **85**, 6175 (1999).
[22] T. Devolder, C. Chappert, V. Mathet, H. Bernas, Y. Chen, J. P. Jarnet, and J. Ferre, J. Appl. Phys. **87**, 8671 (2000).
[23] L. Thomas, S. S. P. Parkin, J. Yu, U. Rüdiger, and A. D. Kent, Appl. Phys. Lett. **76**, 766 (2000).
[24] E. Seynaeve, G. Rens, A. V. Volodin, K. Temst, and C. van Haesendonk, J. Appl. Phys. **89**, 531 (2001).
[25] J. Lohau, A. Carl, S. Kirsch, and E. F. Wassermann, J. Appl. Phys. **78**, 2020 (2001).
[26] E. Gu, E. Ahmad, S. J. Gray, C. Daboo, J. A. C. Bland, L. M. Brown, M. Rührig, A. J. McGibbon, and J. N. Chapman, Phys. Rev. Lett. **78**, 1158 (1997).
[27] J. Raabe, R. Pulwey, R. Sattler, T. Scheinböck, J. Zweck, and D. Weiss, J. Appl. Phys. **88**, 4437 (2000).
[28] W. Wulfhekel, H. F. Ding, and J. Kirschner, J. Appl. Phys. **87**, 6475 (2000).
[29] S. Heinze, M. Bode, A. Kubetzka, O. Pietzsch, X. Nie, S. Blügel, and R. Wiesendanger, Science **288**, 1805 (2000).
[30] O. Pietzsch, A. Kubetzka, M. Bode, and R. Wiesendanger, Phys. Rev. Lett. **84**, 5212 (2000).
[31] S. Pignard, G. Goglio, A. Radulescu, L. Pireaux, S. Dubois, A. Declemy, and J. L. Duvail, J. Appl. Phys. **87**, 824 (2000).
[32] K. L. Chopra, *Thin Film Phenomena* (McGraw-Hill, New York, 1969).
[33] H. Hoffmann, J. Vancea, and U. Jacob, Thin Solid Films **129**, 181 (1985).
[34] J. L. Olsen, *Electron Transport in Metals* (Wiley Interscience, New York/London, 1962).
[35] B. Hausmanns, T. P. Krome, G. Dumpich, E. F. Wassermann, D. Hinzke, U. Nowak, and K. D. Usadel, J. Magn. Magn. Mater. **240**, 297 (2002).
[36] G. Dumpich, T. P. Krome, and B. Hausmanns, J. Magn. Magn. Mater. **248**, 241 (2002).
[37] K. Shigeto, T. Okuno, T. Shinjo, Y. Suzuki, and T. Ono, J. Appl. Phys. **88**, 6636 (2000).
[38] B. Hausmanns, T. P. Krome, and G. Dumpich, J. Appl. Phys. **93**, 8095 (2003).
[39] B. D. Cullity, *Introduction to Magnetic Materials* (Addison-Wesley, Redwood City, CA, 1972).
[40] U. Nowak, in *Annual Reviews of Computational Physics IX*, D. Stauffer (Hrsg.) (World Scientific, Singapore, 2000), p. 105.
[41] D. Hinzke, Ph.D. thesis, University Duisburg, 2002.
[42] S. Hoch, Ph.D. thesis, Ruhr-University Bochum, 2003.
[43] B. Leven, U. Nowak, and G. Dumpich (unpublished).
[44] N. F. Mott, Adv. Phys. **13**, 325 (1964).
[45] A. Fert and C. Vouille, in *Magnetische Schichtsysteme* (Schriften des FZ, Jülich, 1999), p. D1.
[46] J. McCord, R. Schaefer, B. Leven, U. Nowak, and G. Dumpich (unpublished).
[47] U. Nowak, Theoretische Physik, Universität Duisburg-Essen (private communication).
[48] S. Tumanski, *Thin Film Magnetoresistive Sensors* (IOP, Bristol and Philadelphia, 2001).